PAPER

Theoretical modulation of singlet/triplet chemiexcitation of chemiluminescent imidazopyrazinone dioxetanone *via* C$_8$-substitution†

L. Pinto da Silva, [iD] *[a] C. M. Magalhães, [iD] [a] D. M. A. Crista[a] and
J. C. G. Esteves da Silva[a,b]

Coelenterazine, a member of the imidazopyrazinone class of chemiluminescent substrates, presents significant potential as a dynamic probe of reactive oxygen species in a biological environment, such as a superoxide anion, in which these species are important in cellular biology and pathology. The objective of the current study was to understand in what way the efficiency of singlet and triplet chemiexcitation could be modulated, towards a more efficient use of imidazopyrazinone-based compounds as dynamic chemiluminescent probes. To this end the thermolysis of imidazopyrazinone dioxetanone, substituted at the C$_8$-position with electron-donating or electron-withdrawing groups, was characterized with a theoretical approach based on density functional theory. Substituents with different electron-donating/withdrawing characters have only a limited effect on the singlet chemiexcitation of anionic dioxetanone. For neutral dioxetanone, both electron-withdrawing and weak electron-donating substituents increase singlet chemiexcitation, to the contrary of strong electron-donating groups. During their thermolysis reaction, all molecules presented regions of degeneracy with triplet states, thereby indicating the possibility of triplet chemiexcitation.

Introduction

Reactive oxygen species (ROS) are defined as chemical species containing oxygen with high chemical reactivity, which can be produced in biological systems in both enzymatic and non-enzymatic reactions.[1,2] While ROS, including superoxide anions (O$_2$[·−]), are known for their ability to induce harmful effects on cells, they appear to be important signalling molecules in processes ranging from cellular communication to cell division.[3–6] Moreover, it has been discussed that ROS (as O$_2$[·−]) play significant roles in several chronic diseases including cancer, inflammation, and aging,[7–10] besides O$_2$[·−] being a potential biomarker for diabetes mellitus.[11] So, the detection, quantification and imaging of ROS species, particularly of O$_2$[·−], is of the utmost importance. However, there are still few

tools available for studying O$_2$[·−]. Fluorescent probes are available but are optimized for microscopy, and thereby limited to low-throughput *in vitro* or *ex vivo* studies.[11] More importantly, these fluorescent probes are accumulation sensors, and are so unable to provide a dynamic reading of O$_2$[·−].[11,12]

Chemiluminescence-based probes can overcome these problems. Chemiluminescence is considered to be light emission that results from chemical reactions.[13–18] One of the big advantages of chemiluminescence-based sensors is that they do not require excitation sources, meaning that there is no background noise and no problems regarding tissue penetration (except in emission).[11,19,20] More importantly, chemiluminescent probes are not accumulation sensors, but provide a dynamic reading of ROS concentration.[11,19,20] Once the chemiluminescent reaction between the probe and the ROS species occurs and light is emitted, no more photons can be produced from those reactants.

Available chemiluminescent probes for O$_2$[·−] range from luminol to lucigenin, but Coelenterazine shows the highest potential as an O$_2$[·−] probe. Unlike luminol, Coelenterazine exhibits chemiluminescence not dependent on cell-derived myeloperoxidase, and unlike lucigenin, Coelenterazine does not sensitize O$_2$[·−] production (which leads to false-positives).[21–24] In fact, Contag and co-workers have validated

[a]Chemistry Research Unit (CIQUP), Department of Chemistry and Biochemistry, Faculty of Sciences of University of Porto, R. Campo Alegre 687, 4169-007 Porto, Portugal. E-mail: luis.silva@fc.up.pt
[b]Departamento de Geociências, Ambiente e Ordenamento do Território, Faculdade de Ciências da Universidade do Porto, R. Campo Alegre 687, 4169-007 Porto, Portugal
†Electronic supplementary information (ESI) available: Cartesian coordinates of important structures, and orbitals for S$_0$/T$_1$ states at the second intersystem crossing. See DOI: 10.1039/c7pp00012j

This journal is © The Royal Society of Chemistry and Owner Societies 2017

Photochem. Photobiol. Sci., 2017, **16**, 897–907 | 897

the use of Coelenterazine as a chemiluminescent probe for $O_2^{\bullet-}$, both *in vitro* and *in vivo*, in situations of pathology (cancer, chronic inflammation and diabetes mellitus).[11,19,20]

Coelenterazine (Scheme 1) is widely found in many marine organisms (coelenterates, squids, shrimp, fish and copepods).[25–28] This molecule is also part of the imidazopyrazinone-based class of chemiluminescent molecules, which connects many luminescent substrates found in marine organisms (Scheme 1): besides Coelenterazine, there are also *Cypridina* and *Watasenia* luciferins, among others.[29] The luminescent reactions of these imidazopyrazinone molecules have been described as follows: the imidazopyrazinone scaffold reacts with oxidizing agents (as $O_2^{\bullet-}$), which rapidly forms a peroxide that is converted into a four-membered ring: dioxetanone (Scheme 2).[25,29,30] It is the decomposition of dioxetanone that allows a thermally-activated ground state reaction to produce singlet excited state products, which decay latter to the ground state with emission of visible light.[14,15–17,31–37]

While Coelenterazine can be a reliable probe for $O_2^{\bullet-}$, there are some problems that can limit its use as a sensor. While chemiluminescent and bioluminescent systems are known for the generation of singlet excited states, chemiluminescent systems with simpler dioxetanones and dioxetanes are experimentally known for generating triplet state products.[14,15,38,39] While no such experimental data exist for more complex chemiluminescent systems, as imidazopyrazinones and of the

Scheme 1 Chemical structure of imidazopyrazinone and related chemiluminescent compounds.

Scheme 2 Schematic representation of the chemiluminescent reaction of imidazopyrazinone-based compounds.

fireflies (due to the experimental difficulties associated with the study of triplet states), theoretical calculations have shown pathways for triplet chemiexcitation in these systems,[33,35,36] in a similar manner to simpler dioxetanones/dioxetanes. In fact, both our group and that of Isobe and co-workers have shown theoretically that triplet chemiexcitation is possible for the chemiluminescent reactions of imidazopyrazinones.[32,36]

The production of triplet states is problematic due to two main reasons. The first is that as triplet states are very easily quenched, their formation will not be monitored with the luminescent and fluorescent approaches typically used to detect chemiluminescence. Thus, the formation of triplet states has the potential for decreasing the sensibility of the assay. The second problem related with the potential formation of triplet states is that these states are reactive and can produce harmful ROS when interacting with molecular oxygen. This could lead to some problems when using Coelenterazine in biological samples.

Another potential problem is related with singlet chemiexcitation itself. For Coelenterazine to be a suitable $O_2^{\bullet-}$ probe, the resulting light emission should be particularly efficient (especially in water, when thinking of biological samples). However, this is not really the case. First of all, chemiluminescence is already less efficient than the related process, bioluminescence. Moreover, it was found that high contents of water decrease the chemiluminescence efficiency of imidazopyrazinone-based substrates.[40] The chemiluminescence of three different imidazopyrazinone-based derivatives was studied in mixtures of water/*N,N*-dimethylformamide (DMF) and methanol/DMF. It was found that high contents of water greatly decrease the chemiluminescence efficiencies, and that chemiluminescence in methanol/DMF mixtures is much higher than that in water-rich solvents.[40] This can be explained by a decrease in the efficiency of singlet chemiexcitation, as our recent theoretical study revealed that water increases the S_0–S_1 energy gap during imidazopyrazinone dioxetanone thermolysis.[32] Another possibility is a decrease in the fluorescence quantum yield of the emitter, as Shimomura found that the fluorescence of *Cypridina* oxyluciferin is very weak in water.[41]

The objective of this work is to determine how the imidazopyrazinone scaffold of Coelenterazine can be modified, in order to maximize singlet chemiexcitation and limit triplet chemiexcitation in water. To this end, we will study imidazopyrazinone dioxetanone (Scheme 2), the compound responsible for both singlet and triplet chemiexcitation in Coelenterazine and other imidazopyrazinone-based molecules, with different electron-donating ($-NH_2$ and $-CH_3$) and electron-withdrawing ($-CF_3$ and $-CHO$) substituents. Modifications at the C_6-, C_2- and C_8-positions of the imidazopyrazinone scaffold are considered to be the most important in luminescence efficiency.[42,43] Here, we focus on the C_8-position. The substituent effect (at the C_8-position) on the triplet/singlet chemiexcitation of imidazopyrazinone dioxetanone will be studied with a theoretical approach, by performing calculations with density functional theory (DFT) based methods. Theoretical methods have been intensively used with good
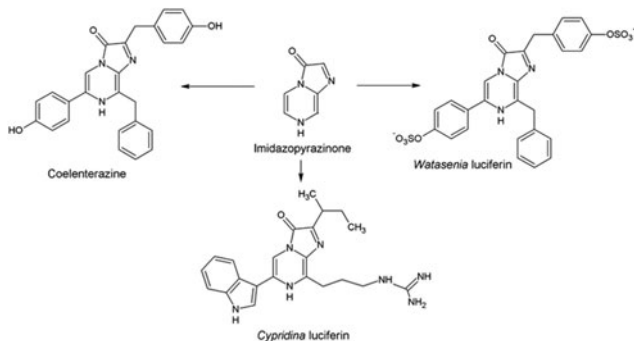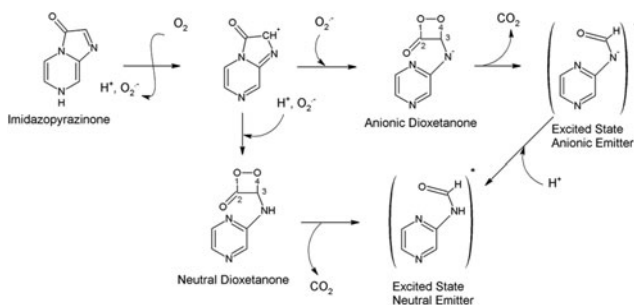
results in bio- and chemiluminescent systems,[44–48] namely in the thermolysis of dioxetanone molecules.[16,17,32–37]

Computational details

The calculations were made with the Gaussian 09 program package.[49] Long-range-corrected hybrid exchange–correlation DFT methods have been gaining importance in the study of dioxetanones due to their ability to provide quite accurate qualitative pictures for these systems.[32–34,50,51] In this study we have employed the ωB97XD long-range corrected functional,[52] as it provides good estimates for $\pi \rightarrow \pi^*$ and $n \rightarrow \pi^*$ local excitation, and CT and Rydberg states.[53] Moreover, it possesses an empirical correction for dealing with dispersion.[52] This functional was already used by us in the study of unsubstituted imidazopyrazinone dioxetanone,[32] facilitating the comparison of new results with the ones obtained before.

Singlet ground state (S_0) geometry optimizations and frequency calculations were performed at the ωB97XD/6-31G(d,p) level of theory, with a closed-shell (R) approach for the reactants and an open-shell (U) one for transition states. The U approach was used with broken-symmetry (BS) technology, which mixes the HOMO and LUMO, making an initial guess for a biradical. Intrinsic reaction coordinates (IRC) were carried out in order to assess if the obtained transition states connected the desired reactants and products.[54] All calculations were made in implicit water by using the Polarizable Continuum Model using the integral equation formalism variant (IEFPCM).[55]

The energies of the S_0 IRC-obtained structures were re-evaluated by single-point calculations at the ωB97XD/6-31+G(d,p) level of theory. The first singlet excited states (S_1) were calculated by using the time dependent (TD) DFT approach,[56] at the TD ωB97XD/6-31+G(d,p) level of theory. The first triplet states (T_1) were calculated on the IRC path geometries with single point energy calculations, at the ωB97XD/6-31+G(d,p) level of theory. These energy re-evaluations were made with U and BS approaches.

The activation energies of these reactions (presented in Table 1) were calculated as follows: frequency calculations at the ωB97XD/6-31G(d,p) level of theory (the same used in the IRC calculations) were performed on the reactant (Tables S9–

S16†) and transition state (Tables S1–S8†) structures, obtained in the IRC calculations, to obtain the correction to the internal thermal energy. The S_0 electronic energies of the reactants and transition states were obtained at the ωB97XD/6-31+G(d,p) level of theory, to which were added the thermal corrections referred before. The activation energies correspond then to the difference, between the reactant and transition states, of this sum of electronic energies and thermal corrections.

To see whether the use of another density functional had any impact in the obtained PES here derived, we have also re-evaluated the S_0 energies at the CAM-B3LYP/6-31+G(d,p) level of theory (Fig. S1 and S2†). CAM-B3LYP[57] is, as ωB97XD, a long-range-corrected functional used previously in the study of imidazopyrazinone-based dioxetanones.[34] The resulting S_0-PES differed very little from the ones obtained with the ωB97XD/6-31+G(d,p) level of theory.

Results and discussion

Reaction mechanism of the thermolysis of substituted imidazopyrazinone dioxetanone

Imidazopyrazinone dioxetanone can be either in a neutral (I-DioxH) or an anionic protonation state (I-Diox⁻), as seen in Scheme 2.[32–37] Thus, in this study we will focus on both forms.

Analysis of Fig. S3 and S4† shows the variation of O_1–O_4 and C_2–C_3 bond lengths during the thermolysis of I-Diox⁻ and I-DioxH, respectively. For all compounds, the reaction begins by cleavage of O_1–O_4, while C_2–C_3 remains constant. Only after the cleavage of O_1–O_4 does the length of C_2–C_3 increases. The involvement of a biradical species is seen by (S^2) values about ~1, for all species.[32,34–36,58] Thus, these thermolysis reactions proceed *via* a stepwise-biradical mechanism. These results are in line with what was observed for firefly dioxetanone, an analogue of *Cypridina* dioxetanone, and unsubstituted I-DioxH/ I-Diox⁻.[32,34–36]

The stepwise-biradical mechanism can be further subdivided: the dioxetanone moiety becomes a radical anion due to an electron transfer (ET) from the electron-rich moiety, which can then be considered as a radical cation; a biradical formed due to the homolytic cleavage of the O_1–O_4 bond. An ET-derived diradical is associated with anionic dioxetanones, while a biradical originating from a homolytic O_1–O_4 breaking is associated with a neutral species.[32–37,58,59]

This trend is maintained for the studied C_8-substituted I-Diox⁻ (Fig. 1), as the spin density resides in the amide nitrogen heteroatom and the two oxygen atoms that form the O_1–O_4 bond. This indicates that this biradical is formed from the breaking of the lone electron pair associated with the ionized amide nitrogen, with one of the electrons being transferred to the dioxetanone moiety.

The spin density of I-DioxH substituted with –CHO, –CF$_3$ and –CH$_3$ groups, is seen only in O_1 and O_4 atoms (indicating a homolytic cleavage of O_1–O_4). For I-DioxH–NH$_2$ the electron spin density is similar to what was obtained for I-Diox⁻ species. Thus, for I-DioxH with electron-withdrawing (–CHO

Table 1 Activation barriers (in kcal mol⁻¹) of the thermolysis reaction of C_8-substituted I-Diox⁻ and I-DioxH, in implicit water. These consist of the difference, between the reactant and transition states, of the sum of electronic energies (at the ωB97XD/6-31+G(d,p) level of theory) and thermal corrections to the energy (at the ωB97XD/6-31G(d,p) level of theory)

Substituent	I-Diox⁻	I-DioxH
–NH$_2$	11.3	20.5
–CH$_3$	12.9	20.9
–CHO	15.7	22.0
–CF$_3$	15.6	21.5

This journal is © The Royal Society of Chemistry and Owner Societies 2017

Photochem. Photobiol. Sci., 2017, **16**, 897–907 | 899
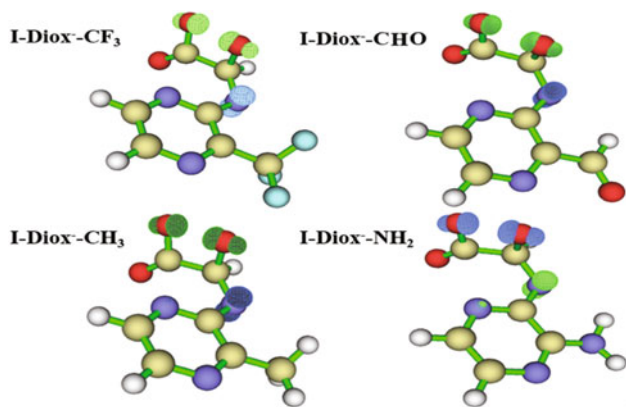
Fig. 1 Representative electron spin density of the biradical generated by the thermolysis of the four C_8-substituted I-Diox⁻ species.

and –CF₃) and weaker electron-donating (–CH₃) substituents, the protonation of the amide nitrogen is sufficient to block an ET-derived thermolysis. However, the addition of strong electron-donating groups as –NH₂ to the C_8-position appears to be sufficient to allow the aminopyrazine moiety of I-DioxH to be involved in an ET process with the peroxide ring.

The decomposition mechanism of the I-Diox⁻ species is very similar to that presented by phenoxyl-substituted 1,2-dioxetanones.[60–62] These reactions are triggered by intramolecular ET from the phenolate group to the peroxide moiety, which is accompanied by peroxide bond breaking, thus generating a biradical anion. The subsequent step is, as in the case of I-Diox⁻, the C–C bond cleavage and the formation of either a radical pair or another radical anion. Thus, this similarity between I-Diox⁻ and phenoxyl-substituted 1,2-dioxetanes indicates that the presence of an ionizable group, when coupled to the peroxide moiety, "forces" the decomposition reaction to occur *via* an ET step.

The comparison between ET- and homolysis-derived mechanisms is supported also by the analysis of the Mulliken atomic charges (Fig. 3 and 4). For I-Diox⁻ (Fig. 3) and I-DioxH–NH₂ species (Fig. 4), significant negative charge transfer (CT) occurs from the aminopyrazine to the dioxetanone moieties, associated with the O_1–O_4 bond breaking, followed by back CT (BCT). For the remaining I-DioxH species (Fig. 4), there is no such CT associated with O_1–O_4 bond breaking. Only a small CT and BCT can be seen at the end of the reaction, most likely associated with the C_2–C_3 bond breaking and the departure of the CO_2 molecule. Such a phenomenon is in line with a recent study regarding an imidazopyrazinone-based dioxetanone.[63]

All C_8-substituted I-Diox⁻ present similar activation barriers, between 11.3 and 15.7 kcal mol⁻¹ (Table 1). These values are in line with a theoretical activation barrier of 13.1 kcal mol⁻¹ for unsubstituted I-Diox⁻ in water,[32] and a theoretical value of 16.0 kcal mol⁻¹ in DMSO for a *Cypridina* dioxetanone analogue.[34] This means that for I-Diox⁻ molecules, the activation barrier is mainly controlled by the ET step from the aminopyrazine core to the peroxide ring, due to the ionization

of the amide nitrogen heteroatom. Nevertheless, electron-donating substituents lead to smaller activation barriers than electron-withdrawing functional groups.

The situation is similar for I-DioxH, with electron-withdrawing substituents leading to higher activation barriers than those presented by molecules with electron-donating groups. The activation barriers of I-DioxH are similar to the theoretical activation energy of 21.0 kcal mol⁻¹ in DMSO, found for a *Cypridina* dioxetanone analogue.[34]

As far as we are aware of, there are still no experimental values for the activation energy of the thermolysis of imidazopyrazinone-based dioxetanones. Thus, we lack experimental values to which we can compare directly the theoretical energies computed here. Nevertheless, the values obtained here for the I-DioxH species are well in line with the experimental results obtained for other dioxetanes and dioxetanones (about 20.0 kcal mol⁻¹).[61,64,65]

Both I-DioxH–CF₃ and I-DioxH–CHO (Fig. 6) present an increase in the energy of the S_0 state right at the end of the flat region of the PES. These correspond to saddle points associated with C_2–C_3 bond breaking. Without thermal effects, the energies are: 25.1 kcal mol⁻¹ for I-DioxH–CF₃, and 24.1 kcal mol⁻¹ for I-DioxH–CHO. Similar points in the S_0 PES were also seen in two recent studies of imidazopyrazinone-based dioxetanones.[34,63]

Singlet chemiexcitation of substituted imidazopyrazinone dioxetanone

In Fig. 5 (I-Diox⁻) and 6 (I-DioxH) are presented the energetic profiles of S_0, S_1 and T_1 states, as a function of intrinsic reaction coordinates in implicit water. We will start by characterizing the singlet chemiexcitation of C_8-substituted I-Diox⁻. It should be noted that these energetic profiles are truncated and the important region of the PES (for chemiexcitation) is enhanced so as to facilitate visualization by the readers. The full profiles are presented in Fig. S5 and S6.†

For –NH₂ substituted I-Diox⁻, the smallest S_0–S_1 energy gap is not smaller than 14.1 kcal mol⁻¹. Moreover, only four IRC points have S_0–S_1 gaps between 14.1 and 15.2 kcal mol⁻¹, with the remaining points presenting gaps significantly higher than 17.0 kcal mol⁻¹. The situation is similar for –CH₃ substituted I-Diox⁻, as only three IRC points present gaps between 14.1 and 15.1 kcal mol⁻¹, with the others presenting gaps significantly higher than 17.1 kcal mol⁻¹. I-Diox⁻–CHO presents slightly higher S_0–S_1 gaps: 14.7, 15.6 and 16.3 kcal mol⁻¹, with the other IRC points presenting gaps higher than 17.4 kcal mol⁻¹. For I-DioxH–CF₃ the situation is even worse, with only two points with energy gaps between 14.8 and 15.4 kcal mol⁻¹.

It should be referred that previous results indicate that multi-reference calculations will surely predict smaller energy gaps between these states.[34,35,50,59,66,67] Previous multi-reference calculations have found in some systems conical intersections between S_0 and S_1 states (as in anionic firefly dioxetanone and 1,2-dioxetanone).[35,59] In other systems (as in Dewar dioxetanone, neutral firefly dioxetanone, thiazole-substituted

900 | *Photochem. Photobiol. Sci.*, 2017, **16**, 897–907

This journal is © The Royal Society of Chemistry and Owner Societies 2017

dioxetanones and 1,2,3,4-dioxetanes), multi-reference calculations predicted S_0–S_1 gaps below ~5 kcal mol^{-1}.[17,35,66,67]

This results from the role of multi-reference correlation in these systems.[51,68] This implies that S_0 and S_1 become nearly degenerate in the biradical region, thus allowing for chemiexcitation. The energetic error present in the biradical region may come from spin contamination in the reference state, introduced by a BS technology.[34,35] However, while multi-reference methods are obviously important to obtain a more quantitative picture of these systems, they may be too computationally demanding to be employed in situations where solvation and more structurally complex systems are involved. Thus, here we have employed a long-rang-corrected hybrid exchange–correlation density functional (ωB97XD), which performs well in predicting local, CT and Rydberg excitation.[52,53] Such a strategy has been gaining importance in chemi-/bioluminescent studies, as such functionals can provide quite accurate qualitative pictures for these systems.[32,34,35,50,69] This is the case here, as the energetic profiles of the S_0 and S_1 states are in line with what was obtained for unsubstituted I-Diox$^-$/I-DioxH and a *Cypridina* dioxetanone analogue.[32,34]

So, our calculations indicate that substituents with electron-donating character should favour S_1 chemiexcitation (when comparing with electron-withdrawing ones), as they decrease the energetic gap between S_0 and S_1. However, the differences induced by different substituents are somewhat limited. In fact, the values here obtained are similar to the ones presented by unsubstituted I-Diox$^-$, in which the smallest S_0–S_1 energy gaps in water were of 14.9 and 12.1 kcal mol^{-1}.[32] For an anionic *Cypridina* dioxetanone analogue the smallest energy gaps (*in vacuo*) were of 16.2 and 12.9 kcal mol^{-1},[34] and 17.7 and 15.0 kcal mol^{-1} for the amide species of *W. scintillans* dioxetanone.[63] Given this, the conclusion is that the presence of an ionized amide group "dominates" the singlet chemiexcitation mechanism, which results in a limited effect provided by the electronic character of the substituents. Such a conclusion is similar to what was found for the activation barrier in the S_0 state. It should be noted that this is in line with some experimental results, in which the authors have stated that for anionic imidazopyrazinone-based dioxetanones, the substituent effects had little effect on the singlet chemiexcitation yield.[70–72]

Having analysed the singlet chemiexcitation for C_8-substituted I-Diox$^-$ in water, we have studied the same process for I-DioxH (Fig. 6). For the sake of comparison, it should be noted that the S_0–S_1 energy gap of unsubstituted I-DioxH in water was always higher than 16.2 kcal mol^{-1}, except an IRC point with a gap of 6.1 kcal mol^{-1}. For I-DioxH–NH$_2$ the situation was similar to that of unsubstituted I-DioxH, as the S_0–S_1 energy gap was always higher than 16.3 kcal mol^{-1}. However, no point with a gap of 6.1 kcal mol^{-1} (or similar) was found. Thus, the efficiency for singlet chemiexcitation of I-DioxH–NH$_2$ is apparently worse than for I-DioxH, and similar to that of I-Diox$^-$ species studied here and elsewhere.[32,34,63]

On the contrary, both electron-withdrawing substituents (–CHO and –CF$_3$) and weaker electron-donating substituents

(–CH$_3$) appear to improve significantly the singlet chemiexcitation of I-DioxH in water (Fig. 6). Upon entering the biradical region provoked by O_1–O_4 bond breaking, both S_0 and S_1 states enter a flat and long region of the PES, where both states can be considered to be nearly-degenerate (given the small S_0–S_1 energy gap). The S_0–S_1 energy gap of I-DioxH–CF$_3$ is between 8.7 and 13.8 kcal mol^{-1}, while the energy gap of I-DioxH–CHO is even smaller: between 6.0 and 13.8 kcal mol^{-1}. For I-DioxH–CH$_3$, the gap is between 10.9 and 13.3 kcal mol^{-1} followed later in the PES by a gap of 9.4 kcal mol^{-1}.

This phenomenon results from the occurrence of a flat region of the PES, which can be accessed by the bond breaking of O_1–O_4 (Fig. 6). Such a region of the PES has been denominated by several authors as an "entropic trap", and has been associated with the decomposition of neutral dioxetanones.[34,35,58,63,66,67] According to these authors, the flatness of the PES compels the reacting molecules to spend a long time passing through this region, which given its near degeneracy with S_1 provides a significant probability of a nonadiabatic transition between S_0 and S_1.[34,35,58,63,66,67] In our previous study of unsubstituted I-DioxH and I-Diox$^-$, our results indicated that this flat region of the PES can only be accessed *via* a homolytic O_1–O_4 bond breaking (and not an ET-derived one), with limited CT between the dioxetanone and aminopyrazine moieties.[32] This is supported in this study, given that this flat region was only accessed by I-DioxH–CF$_3$, I-DioxH–CHO and I-DioxH–CH$_3$, in which O_1–O_4 bond breaking occurred *via* homolysis with limited CT (Fig. 2 and 4). This was not the case for I-DioxH–NH$_2$ and I-Diox$^-$ species (Fig. 1–4), in which O_1–O_4 bond breaking occurs with significant CT and *via* an ET step.

It should be noted that an alternative explanation to "entropic trapping" can be formulated here, based on the energy barriers (associated with C_2–C_3 bond breaking) referred previously. These energy barriers were only found for I-DioxH–CF$_3$ and I-DioxH–CHO, and not for other species (as I-DioxH–CH$_3$). The presence of these barriers at the end of the flat region of the PES means that the reaction intermediates will take more
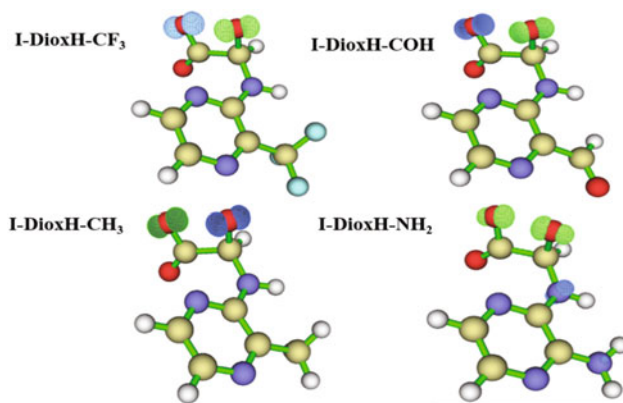

Fig. 2 Representative electron spin density of the biradical generated by the thermolysis of the four C_8-substituted I-DioxH species.

This journal is © The Royal Society of Chemistry and Owner Societies 2017

Photochem. Photobiol. Sci., 2017, **16**, 897–907 | 901

Fig. 3 Mulliken charge density evolution of the dioxetanone and aminopyrazine moieties, during the thermolysis of the four C_8-substituted I-Diox$^-$ species.
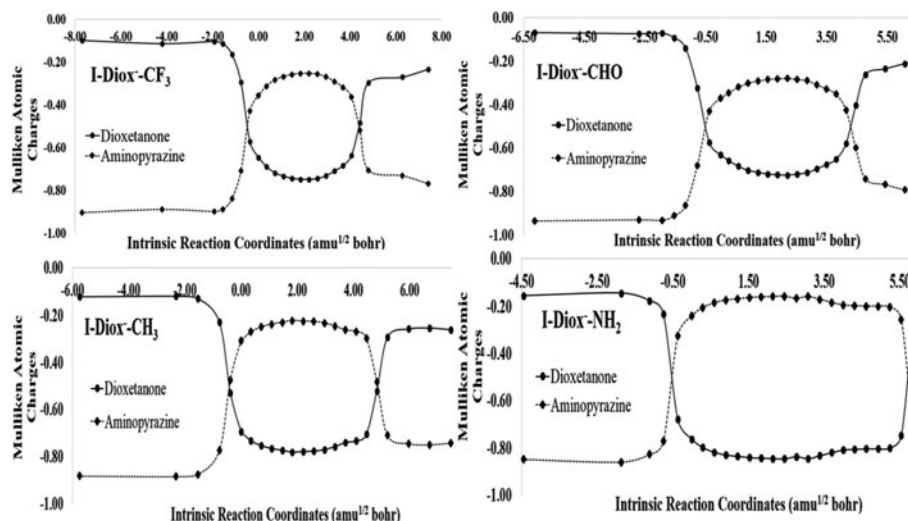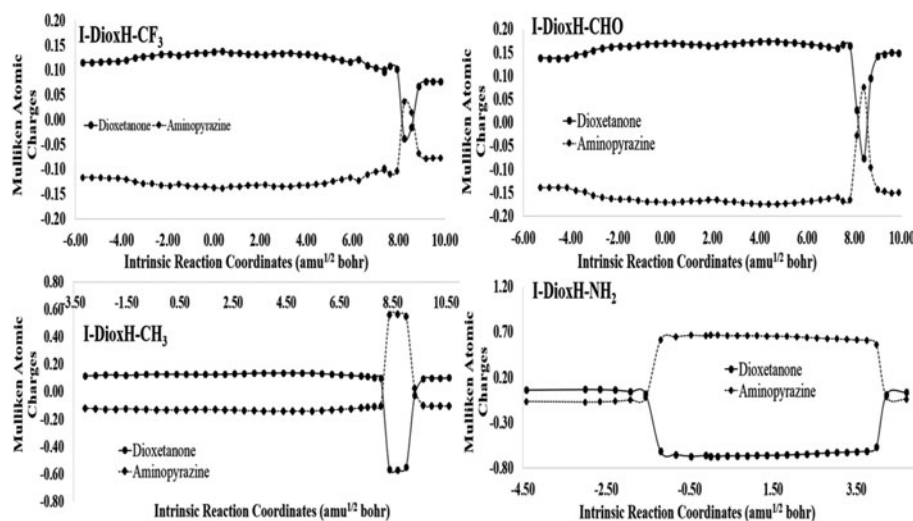

Fig. 4 Mulliken charge density evolution of the dioxetanone and aminopyrazine moieties, during the thermolysis of the four C_8-substituted I-DioxH species.

time to exit that region, before full thermolysis takes place. That would force the reacting molecules to spend more time in the region of the PES where singlet/triplet chemiexcitation is possible, leading to more efficient chemiexcitation without the need of invoking concepts as "entropic trap". Thus, the efficiency of chemiexcitation would depend on the existence and height of this barrier.

In this study this would mean that, despite the existence of all three molecules of a flat region of the PES where S_0 and S_1 are near-degenerate, the efficiency of singlet chemiexcitation increases in the following order: I-DioxH–CH$_3$ (no C_2–C_3 energy barrier) < I-DioxH–CHO (energy barrier of 4.5 kcal mol^{-1}) < I-DioxH–CF$_3$ (energy barrier of 5.4 kcal mol^{-1}). These energy barriers were obtained by calculating the S_0

electronic energy difference between the reacting intermediates and the C_2–C_3 saddle points (Fig. 6).

In conclusion, addition of electron-withdrawing and weak electron-donating substituents to the C_8-position increases singlet chemiexcitation of I-DioxH, by allowing it to access the flat region of the PES that is nearly degenerate with S_1, as their electronic character does not suffice for the O_1–O_4 bond breaking to occur with significant CT and ET.

Triplet chemiexcitation of substituted imidazopyrazinone dioxetanone

As in line with several theoretical and experimental studies on dioxetanones, dioxetanes and dioxetanedione, we have found pathways for triplet chemiexcitation in both C_8-substituted

902 | *Photochem. Photobiol. Sci.*, 2017, **16**, 897–907

This journal is © The Royal Society of Chemistry and Owner Societies 2017

I-Diox⁻ and I-DioxH (Fig. 5 and 6).[32,35–39,58,59,67] In all cases, with the evolution of dioxetanone thermolysis, S_0 and T_1 become degenerate/nearly-degenerate and even cross in different points of the reaction. This signalizes the existence of two intersystem crossings, which is in line with what was seen previously for unsubstituted I-Diox⁻ and I-DioxH.[32,36]

Nevertheless, some differences can be seen. While all I-Diox⁻ species present very similar S_0–T_1 energy gaps (∼0 to ∼8 kcal mol⁻¹), the extension of this region of the PES depends on the electronic character of the substituent. The addition of both electron-donating/withdrawing characters decreases the length of this region when compared with unsubstituted I-Diox⁻.[32] However, the addition of electron-withdrawing substituents to I-Diox⁻ decreases more the length

of this region of the PES, than the addition of electron-donating groups.

As for the case of substituted I-Diox⁻, the addition of substituents to I-DioxH did not affect the energy values of the S_0–T_1 energy gap, but only the length of the PES region in which the states are degenerate/near-degenerate. Both electron-withdrawing and weak electron-donating substituents increase the length of this region, while strong electron-donating substituents decrease it.

It should be noted that as intersystem crossing is a process formally forbidden in non-relativistic quantum theory, inferring singlet–triplet transition probability only from energy gaps is not sufficiently accurate.[73,74] In fact, for these transitions to become allowed, vibrational factors must be coupled to electronic selec-
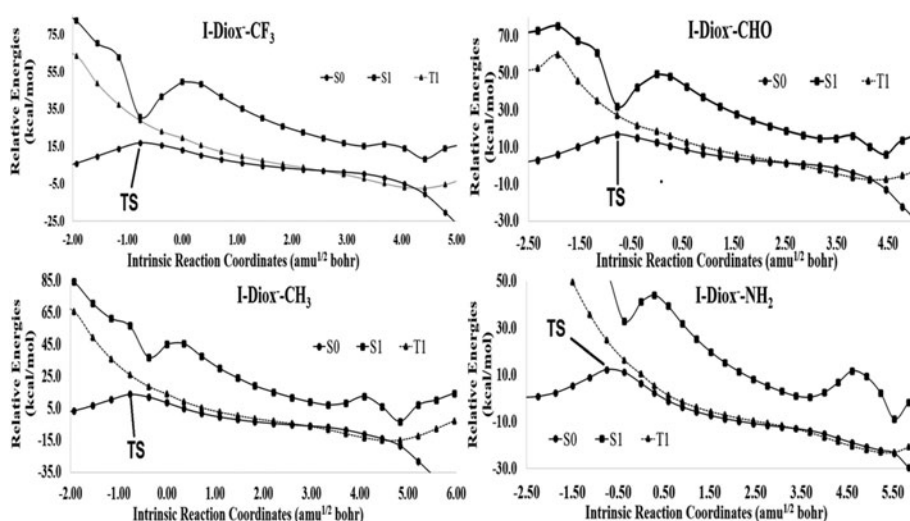

Fig. 5 Energy profiles of the S_0, S_1 and T_1 states during the thermolysis of the four C_8-substituted I-Diox⁻ species, in water. This is the truncated version, enhancing the region where chemiexcitation occurs. For the full version of the PES, see Fig. S5.†

Fig. 6 Energy profiles of the S_0, S_1 and T_1 states during the thermolysis of the four C_8-substituted I-DioxH species, in water. This is the truncated version, enhancing the region where chemiexcitation occurs. For the full version of the PES, see Fig. S6.†
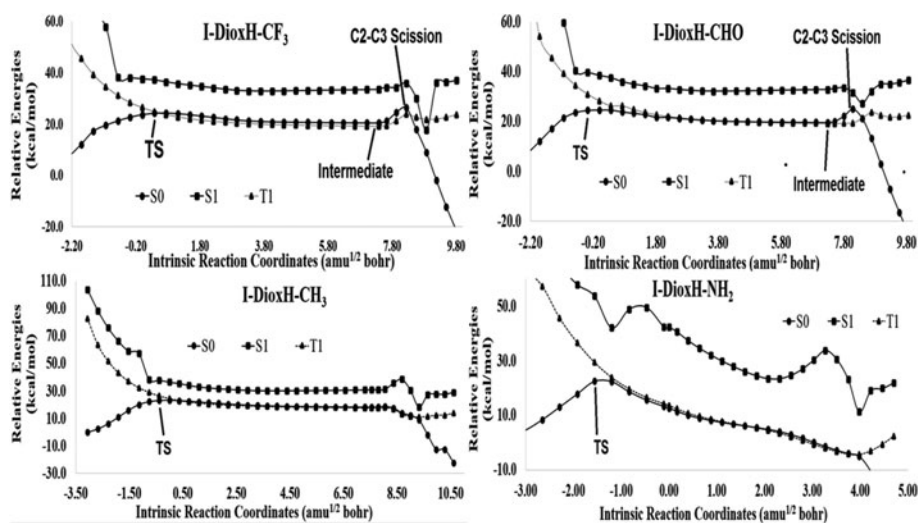
This journal is © The Royal Society of Chemistry and Owner Societies 2017

Photochem. Photobiol. Sci., 2017, 16, 897–907 | 903

tion rules. So, for a more quantitative discussion, spin–orbit couplings should be computed at a multi-reference level. However, as discussed previously, multi-reference methods require too much computational power for their use to be feasible on these structurally complex more systems and in situations where solvation is included.[32,34,63] This is particularly true as the use of small active spaces is not advisable, as previous work of different authors demonstrated that active spaces of at least 16 electrons in 13 orbitals are required for a realistic depiction of the thermolysis and chemiexcitation of dioxetanone species.[35,51,59,75] Even other authors who have used smaller active spaces, never used the ones smaller than 12 electrons in 10 orbitals.[17,67]

Alternatively, we can also take into account the El-Sayed rules for a more qualitative assessment of intersystem crossing rates. The El-Sayed rules state that the rate of intersystem crossing is relatively large if the transition involves a change of orbital type.[73,76] Thus, we have compared the HOMO and LUMO, of the S_0 state, to the SOMO(1) and SOMO(2), of the T_1 state, respectively. This was made for each species at the co-ordinates corresponding to the two intersystem crossings. The corresponding orbitals are presented in Fig. S7–S22.† These are natural orbitals calculated with Gaussian 09,[49] but which are visualized through the Multiwfn software.[77]

Analysis of these figures shows that the orbital type is not significantly different for all the considered molecules. Even in cases were a bit of π-electron density disappears, the corresponding orbitals still remain with significant σ-character. Thus, the only conclusion that can be reached by this analysis is that these intersystem crossings should not have very large rate constants.

In conclusion, the analysis of the S_0–T_1 energy gaps indicates that there is a possibility for intersystem crossing in these molecules. This is in line with experimental studies of simpler dioxetane and dioxetanone molecules that showed that their thermolysis leads mainly to triplet state products (with quantum yields up to 30%), while singlet chemiexcitation rarely reaches 1%.[39,78–80] However, analysis taking into account the El-Sayed rules,[73,76] indicates that the rates of the intersystem crossings should not have very large rate constants. Nevertheless, the spin-forbidden and multi-reference character of S_0–T_1 transitions makes it difficult to provide more than qualitative information regarding such transitions in the molecules studied here, at the current level of theory. Thus, further study regarding triplet chemiexcitation is needed.

Conclusions

Our results have indicated that electron-donating or electron-withdrawing substituents at the C_8-position have only a limited influence on the activation barrier of both the anionic and neutral forms of imidazopyrazinone dioxetanone. Nevertheless, electron-donating substituents decrease the activation barrier while electron-withdrawing substituents increase it.

The electronic character of the substituents also has little effect on the singlet chemiexcitation of the anionic form of imidazopyrazinone dioxetanone. Both the results regarding singlet chemiexcitation and the activation barrier of the anionic species indicate that these processes are already dependent on CT/ET steps originating from the ionized amide nitrogen, thereby being only slightly affected by the electronic character of the substituents.

However, this is not the case for the neutral form of dioxetanone. Electron-withdrawing and weak electron-donating substituents improve significantly the efficiency of singlet chemiexcitation. The addition of these substituents allows the access to a flat region of the PES, where the singlet ground and excited states are nearly-degenerate.

Such a region of the PES can be accessed if the peroxide bond breaking occurs *via* homolysis, without significant charge transfer between the dioxetanone and the aminopyrazine moieties. As the addition of strong electron-donating substituents induces both significant charge and electron transfer processes, they are not able to access the flat region of the PES in which the ground and excited singlet states are nearly-degenerate, thereby decreasing singlet chemiexcitation.

As for triplet chemiexcitation, the thermolysis of both the anionic and neutral forms of imidazopyrazinone dioxetanone, with both electron-donating and electron-withdrawing substituents, provide regions of significant degeneracy between the singlet ground and first triplet excited states. Thus, triplet chemiexcitation appears to be a factor that must be taken into account when dealing with imidazopyrazinone-based dioxetanones. However, the spin-forbidden and multi-reference nature of intersystem crossing makes it difficult to provide a quantitative assessment of the singlet–triplet transitions involving the molecules studied here.

Acknowledgements

Notes and references

1 T. R. Figueira, M. H. Barros, A. A. Camargo, R. F. Castilho, J. C. B. Ferreira, A. J. Kowaltoski, F. E. Sluse, N. C. Souza-Pinto and A. E. Vercesi, Mitochondria as a Source of

904 | *Photochem. Photobiol. Sci.*, 2017, **16**, 897–907

This journal is © The Royal Society of Chemistry and Owner Societies 2017

Reactive Oxygen and Nitrogen Species: From Molecular Mechanisms to Human Health, *Antioxid. Redox Signaling*, 2013, **18**, 2029.

2 H. Pelicano, D. Carney and P. Huang, ROS stress in cancer cells and therapeutic implications, *Drug Resist. Updates*, 2004, **7**, 97.

3 W. C. Burhans and N. H. Heintz, The cell cyclic is a redox cycle: Linking phase-specific targets to cell fate, *Free Radical Biol. Med.*, 2009, **47**, 1282.

4 A. B. Fisher, Redox signaling across cell membranes, *Antioxid. Redox Signaling*, 2009, **11**, 1349.

5 P. D. Ray, B. W. Huang and Y. Tsuji, Reactive oxygen species (ROS) homeostasis and redox regulation in cellular signaling, *Cell Signalling*, 2012, **24**, 981.

6 B. C. Dickinson and C. J. Chang, Chemistry and biology of reactive oxygen species in signaling or stress responses, *Nat. Chem. Biol.*, 2011, **7**, 504–511.

7 G. Waris and H. Ahsan, Reactive oxygen species: role in the development of cancer and various chronic conditions, *J. Carcinog.*, 2006, **5**, 14.

8 H. P. Indo, H. C. Yen, I. Nakanishi, K. Matsumoto, M. Tamura, Y. Nagano, H. Matsui, O. Gusev, R. Cornette, T. Okuda, Y. Minamiyama, H. Ichikawa, S. Suenaga, M. Oki, T. Sato, T. Ozawa, D. K. St. Clair and H. J. Majima, A mitochondrial superoxide theory for oxidative stress diseases and aging, *J. Clin. Biochem. Nutr.*, 2015, **56**, 1.

9 T. Finkel and N. J. Holbrook, Oxidants, oxidative stress and the biology of ageing, *Nature*, 2000, **408**, 239.

10 R. Fischer and O. Maier, Interrlation of Oxidative Stress and Inflammation in Neurodegenerative Disease: Role of TNF, *Oxid. Med. Cell. Longevity*, 2015, **2015**, 1.

11 L. L. Bronsart, C. Stokes and C. H. Contag, Chemiluminescence imaging of superoxide anion detects beta-cell function and mass, *PLoS One*, 2016, **11**, e0146601.

12 R. R. Nazarewicz, A. Bikineyeva and S. I. Dikalov, Rapid and specific measurements of superoxide using fluorescence spectroscopy, *J. Biomol. Screening*, 2013, **18**, 498.

13 C. M. Magalhães, J. C. G. Esteves da Silva and L. Pinto da Silva, Chemiluminescence and bioluminescence as an excitation source in the photodynamic therapy of cancer: a critical review, *ChemPhysChem*, 2016, **17**, 2286.

14 I. Navizet, Y. J. Liu, N. Ferré, D. Roca-Sanjuán and R. Lindh, The chemistry of bioluminescence: an analysis of chemical functionalities, *ChemPhysChem*, 2011, **12**, 3064.

15 L. Pinto da Silva and J. C. G. Esteves da Silva, Firefly chemiluminescence and bioluminescence: efficient generation of excited states, *ChemPhysChem*, 2012, **13**, 2257.

16 C. Tanaka, J. Tanaka and M. Matsumoto, An intramolecular charge/electron transfer chemiluminescence mechanism of oxidophenyl-substituted 1,2-dioxetane, *Phys. Chem. Chem. Phys.*, 2011, **13**, 16005–16014.

17 P. Farahani, M. Lundberg, R. Lindh and D. Roca-Sanjuan, Theoretical study of the dark photochemistry of 1,3-butadiene *via* the chemiexcitation of Dewar dioxetanes, *Phys. Chem. Chem. Phys.*, 2015, **17**, 18653–18664.

18 S. Schramm, I. Navizet, P. Naumov, N. K. Nath, R. Berraud-Pache, P. Oesau, D. Weiss and R. Beckert, The light emitter of the 2-coumarone chemiluminescence: theoretical and experimental elucidation of a possible model for bioluminescent systems, *Eur. J. Org. Chem.*, 2016, 678.

19 L. L. Bronsart, C. Stokes and C. H. Contag, Multimodality imaging of cancer superoxide anion using the small molecule Coelenterazine, *Mol. Imaging Biol.*, 2016, **18**, 166.

20 L. L. Bronsart, L. Nguyen, A. Habtezion and C. H. Contag, Reactive oxygen species imaging in a mouse model of inflammatory bowel disease, *Mol. Imaging Biol.*, 2016, **18**, 473.

21 M. Kervinen, J. Patsi, M. Finel and I. E. Hassinen, Lucigenin and Coelenterazine as superoxide probes in mitochondrial and bacterial membranes, *Anal. Biochem.*, 2004, **324**, 45.

22 S. I. Liochev and I. Fridovich, Lucigenin (Bis-N-methylacridinium) as a mediator of superoxide anion production, *Arch. Biochem. Biophys.*, 1997, **337**, 115.

23 M. M. Tarpey, C. R. White, E. Suarez, G. Richardson, R. Radi and B. Freeman, Chemiluminescent detection of oxidants in vascular tissue - Lucigenin but not Coelenterazine enhances superoxide formation, *Circ. Res.*, 1999, **84**, 1203.

24 L. Zhang, L. Yu and C. A. Yu, Generation of superoxide anion by succinate-cytochrome c reductase from bovine heart mitochondria, *J. Biol. Chem.*, 1998, **273**, 33972.

25 Z. M. Kaskova, A. S. Tsarkova and I. V. Yampolsky, 1001 lights: luciferins, luciferases, their mechanisms of action and applications in chemical analysis, biology and medicine, *Chem. Soc. Rev.*, 2016, **45**, 6048.

26 O. Shimomura, S. Inoue, F. H. Johnson and Y. Haneda, Widespread occurrence of Coelenterazine in marine bioluminescence, *Comp. Biochem. Physiol.*, 1980, **65B**, 435.

27 J. F. Rees, E. M. Thompson, F. Baguet and F. I. Tsuji, Detection of Coelenterazine and related luciferase activity in the tissues of the luminous fish, *vinciguerria-attenuata*, *Comp. Biochem. Physiol.*, 1990, **96A**, 425.

28 A. K. Campbell and P. J. Herring, Imidazolopyrazine bioluminescence in copepods and other marine organisms, *Mar. Biol.*, 1990, **104**, 219.

29 K. Teranishi, Luminescence of imidazo[1,2-a]pyrazine-3 (7H)-one compounds, *Bioorg. Chem.*, 2007, **35**, 82.

30 T. Jiang, L. Du and M. Li, Lighting up bioluminescence with Coelenterazine: strategies and applications, *Photochem. Photobiol. Sci.*, 2016, **15**, 466.

31 Y. Ishii, C. Hayashi, Y. Suzuki and T. Hirano, Chemiluminescent 2,6-diphenylimidazo[1,2-a]pyrazine-3 (7H)-ones: a new entry to Cypridina luciferin analogues, *Photochem. Photobiol. Sci.*, 2014, **13**, 182.

32 L. Pinto da Silva, C. M. Magalhães and J. C. G. Esteves da Silva, Interstate Crossing-Induced Chemiexcitation Mechanism as the Basis for Imidazopyrazinone Bioluminescence, *ChemistrySelect*, 2016, **1**, 3343.

33 H. Isobe, Y. Takano, M. Okumura, S. Kuramitsu and Y. Yamaguchi, Mechanistic insights in charge-transfer-

This journal is © The Royal Society of Chemistry and Owner Societies 2017

Photochem. Photobiol. Sci., 2017, **16**, 897–907 | 905

induced luminescence of 1,2-dioxetanones with a substituent of low oxidation potential, *J. Am. Chem. Soc.*, 2005, **127**, 8667–8679.

34 B. W. Ding, P. Naumov and Y. J. Liu, Mechanistic insight into marine bioluminescence: photochemistry of the chemiexcited Cypridina (sea firefly) lumophore, *J. Chem. Theory Comput.*, 2015, **11**, 591.

35 L. Yue, Y. J. Liu and W. H. Fang, Mechanistic insight into the chemiluminescent decomposition of firefly dioxetanone, *J. Am. Chem. Soc.*, 2012, **134**, 11632.

36 H. Isobe, S. Yamanaka, S. Kuramitsu and K. Yamaguchi, Regulation mechanism of spin-orbit coupling in charge-transfer-induced luminescence of imidazopyrazinone derivatives, *J. Am. Chem. Soc.*, 2008, **130**, 132.

37 L. Pinto da Silva and J. C. G. Esteves da Silva, Interstate Crossing-Induced Chemiexcitation as the Reason for the Chemiluminescence of Dioxetanones, *ChemPhysChem*, 2013, **14**, 1071.

38 M. Matsumoto, Advanced chemistry of dioxetanes-based chemiluminescent substrates originating from bioluminescence, *J. Photochem. Photobiol., C*, 2004, **5**, 27.

39 W. Adam and W. J. Baader, Effets of methylation on the thermal-stability and chemi-luminescence properties of 1,2-dioxetanes, *J. Am. Chem. Soc.*, 1985, **107**, 410.

40 K. Teranishi, M. Hisamatsu and T. Yamada, Chemiluminescence of 2-methyl-6-arylimidazo[1,2-a]pyrazine-3(7H)-one in protic solvents: electron-donating substituent effect on the formation of the neutral singlet excited-state molecule, *Luminescence*, 1999, **14**, 297.

41 O. Shimomura, F. H. Johnson and T. Masugi, Cypridina bioluminescence - light-emitting oxyluciferin-luciferase complex, *Science*, 1969, **164**, 1299.

42 T. Jiang, X. Yang, X. Yang, M. Yuan, T. Zhang, H. Zhang and M. Li, Novel bioluminescent Coelenterazine derivatives with imidazopyrazinone C-6 extended substitution for Renilla luciferase, *Org. Biomol. Chem.*, 2016, **14**, 5272.

43 R. Nishihara, H. Suzuki, E. Hoshino, S. Suganuma, M. Sato, T. Saitoh, S. Nishiyama, N. Iwasawa, D. Citterio and K. Suzuki, Bioluminescent coelenterazine derivatives with imidazopyrazine C-6 extended substitution, *Chem. Commun.*, 2015, **51**, 391.

44 R. Berraud-Pache and I. Navizet, QM/MM calculations on a newly synthesized oxyluciferin substrate: new insights into the conformation effect, *Phys. Chem. Chem. Phys.*, 2016, **18**, 27460.

45 B. F. Milne, Red-shifting the optical response of firefly oxyluciferin with group 15/16 substitutions, *Phys. Chem. Chem. Phys.*, 2014, **16**, 24971.

46 C. G. Min, Y. Leng, X. K. Yang, S. J. Huang and A. M. Ren, Systematic color tuning of a family of firefly oxyluciferin analogues suitable for OLED applications, *Dyes Pigm.*, 2016, **126**, 202.

47 L. Pinto da Silva and J. C. G. Esteves da Silva, Chemiexcitation induced proton transfer: enolate oxyluciferin as the firefly bioluminophore, *J. Phys. Chem. B*, 2015, **119**, 2140.

48 D. Roca-Sanjuán, M. G. Delcey, I. Navizet, N. Ferré, Y. J. Liu and R. Lindh, Chemiluminescence and fluorescence states of a small model for coelenteramide and cypridina oxyluciferin: a CASSCF/CASPT2 study, *J. Chem. Theory Comput.*, 2011, **7**, 4060–4069.

49 M. J. Frisch, *et al.*, *Gaussian 09, Revision A.02*, Gaussian, Inc., Wallingford CT, 2009.

50 L. Yue and Y. J. Liu, Mechanism of AMPPD chemiluminescence in a different voice, *J. Chem. Theory Comput.*, 2013, **9**, 2300.

51 L. Greenman and D. A. Mazziotti, Strong electron correlation in the decomposition reaction of dioxetanone with implications for firefly bioluminescence, *J. Chem. Phys.*, 2010, **133**, 164110.

52 J. D. Chai and M. Head-Gordon, Long-range corrected hybrid density functionals with damped atom-atom dispersion corrections, *Phys. Chem. Chem. Phys.*, 2008, **10**, 6615.

53 C. Adamo and D. Jacquemin, The calculations of excited-state properties with Time-Dependent Density Functional Theory, *Chem. Soc. Rev.*, 2013, **42**, 845.

54 H. P. Hratchian and H. B. Schlegel, Using Hessian updating to increase the efficiency of a Hessian based predictor-corrector reaction path following method, *J. Chem. Theory Comput.*, 2005, **1**, 61.

55 J. Tomasi, B. Mennucci and R. Cami, Quantum mechanical continuum solvation models, *Chem. Rev.*, 2005, **105**, 2999.

56 G. Scalmani, M. J. Frisch, B. Mennucci, J. Tomasi, R. Cammi and V. Barone, Geometries and properties of excited states in the gas phase and in solution: Theory and application of a time-dependent density functional theory polarizable continuum model, *J. Chem. Phys.*, 2006, **124**, 094107.

57 T. Yanai, D. P. Tew and N. C. Handy, A new hybrid exchange-correlation functional using the Coulomb-attenuating method (CAM-B3LYP), *Chem. Phys. Lett.*, 2004, **393**, 51.

58 L. Pinto da Silva and J. C. G. Esteves da Silva, Mechanistic study of the unimolecular decomposition of 1,2-dioxetanedione, *J. Phys. Org. Chem.*, 2013, **26**, 659.

59 F. Liu, Y. J. Liu, L. De Vico and R. Lindh, *J. Am. Chem. Soc.*, 2009, **131**, 6181.

60 F. A. Augusto, G. A. Souza, S. P. Souza Júnior, M. Khalid and W. J. Baader, Efficiency of electron transfer initiated chemiluminescence, *Photochem. Photobiol.*, 2013, **89**, 1299.

61 A. L. P. Nery, S. Ropke, L. H. Catalani and W. J. Baader, Fluoride-triggered decomposition of m-silyloxyphenyl-substituted dioxetanes by an intramolecular electron transfer (CIEEL) mechanism, *Tetrahedron Lett.*, 1999, **40**, 2443.

62 L. F. M. L. Ciscato, F. H. Bartoloni, D. Weiss, R. Beckert and W. J. Baader, Experimental evidence of the occurrence of intramolecular electron transfer in catalyzed 1,2-dioxetane decomposition, *J. Org. Chem.*, 2010, **75**, 6574.

63 B. W. Ding and Y. J. Liu, Bioluminescence of firefly squid via mechanism of single-electron-transfer oxygenation and

906 | *Photochem. Photobiol. Sci.*, 2017, **16**, 897–907

This journal is © The Royal Society of Chemistry and Owner Societies 2017

charge-transfer-induced luminescence, *J. Am. Chem. Soc.*, 2017, **139**, 1106.

64 M. Matsumoto, Y. Ito, M. Murakami and N. Watanabe, Synthesis of 5-tert-butyl-1-(3-tert-butyldimethylsiloxy)phenyl-4,4-dimethyl-2,6,7-trioxabicyclo[3.2.0]heptanes and their fluoride-induced chemiluminescent decomposition: effect of a phenolic electron donor on the CIEEL decay rate in aprotic polar solvent, *Luminescence*, 2002, **17**, 305.

65 M. Tanimura, N. Watanabe, H. K. Ijuin and M. Matsumoto, Intramolecular charge-transfer-induced decomposition promoted by an aprotic polar solvent for bicyclic di-oxetanes bearing a 4-(benzothiazol-2-yl)-3-hydroxyphenyl moiety, *J. Org. Chem.*, 2011, **76**, 902.

66 F. Liu, Y. J. Liu, L. De Vico and R. Lindh, A CASSCF/CASPT2 approach to the decomposition of thiazole-substituted di-oxetanone. Substitution effects and charge-transfer induced electron excitation, *Chem. Phys. Lett.*, 2009, **484**, 69.

67 L. De Vico, Y. J. Liu, J. W. Krogh and R. Lindh, Chemiluminescence of 1,2-dioxetane. Reaction mechanism uncovered, *J. Phys. Chem. A*, 2007, **111**, 8013.

68 J. J. Foley, A. E. Rothman and D. A. Mazziotti, Strongly correlated mechanisms of a photoexcited radical reaction from the anti-Hermitian contracted Schrodinger equation, *J. Chem. Phys.*, 2011, **134**, 034111.

69 C. Hou, Y. J. Liu, N. Ferré and W. H. Fang, Understanding bacterial bioluminescence: a theoretical study of the entire process, from reduced Flavin to light emission, *Chem. – Eur. J.*, 2014, **20**, 7979.

70 T. Hirano, Y. Takahashi, H. Kondo, S. Maki, S. Kojima, H. Ikeda and H. Niwa, The reaction mechanism for the high quantum yield of Cypridina (Vargula) bio-luminescence supported by the chemiluminescence of 6-aryl-2-methylimidazo[1,2-a]pyrazin-3(7H)-ones (Cypridina luciferin analogues), *Photochem. Photobiol. Sci.*, 2008, **7**, 197.

71 Y. Takahashi, H. Kondo, S. Maki, H. Niwa, H. Ikeda and T. Hirano, Chemiluminescence of 6-aryl-2-methylimidazo[1,2-a]pyrazine-3(7H)-ones in DMSO/TMG and in diglyme/acetate buffer: support for the chemiexcitation process to generate the singlet-excited state of neutral oxyluciferin in a high quantum yield in the Cypridina (Vargula) bio-luminescence mechanism, *Tetrahedron Lett.*, 2006, **47**, 6057.

72 R. Saito, T. Hirano, S. Maki and H. Niwa, Synthesis and chemiluminescent properties of 6,8-diaryl-2-methylimidazo[1,2-alpha]pyrazin-3(7H)-ones: systematic investigation of substituent effect at para-position of phenyl group at 8-position, *J. Photochem. Photobiol., A*, 2014, **293**, 12.

73 C. M. Marian, Spin-orbit coupling and intersystem crossing in molecules, *WIRES Comput. Mol.*, 2012, **2**, 187.

74 R. Englman and J. Jortner, Energy gap law for radiationless transitions in large molecules, *Mol. Phys.*, 1970, **18**, 145.

75 L. Greenman and D. A. Mazziotti, Balancing single- and multi-reference correlation in the chemiluminescent reaction of dioxetanone using the anti-Hermitian contracted Schrodinger equation, *J. Chem. Phys.*, 2011, **134**, 174110.

76 M. A. El-Sayed, Spin-orbit coupling and the radiationless processes in nitrogen heterocyclics, *J. Chem. Phys.*, 1963, **38**, 2834.

77 T. Lu and F. Chen, Multiwfn: A multifunctional wavefunction analyzer, *J. Comput. Chem.*, 2012, **33**, 580.

78 S. P. Schmidt and G. B. Schuster, Kinetics of unimolecular dioxetanone chemiluminescence - competitive parallel reaction paths, *J. Am. Chem. Soc.*, 1978, **100**, 5559.

79 A. L. P. Nery and W. J. Baader, Chemiluminescence of cyclic organic peroxides: generation of electronically excited states in 1,2-dioxetane decomposition, *Quim. Nova*, 2001, **24**, 626.

80 W. Adam, Thermal generation of electronic excitation with hyperenergetic molecules, *Pure Appl. Chem.*, 1980, **52**, 2591.